

PICTORIAL ESSAY

Musculoskeletal imaging

Anterior knee pain in paediatrics: Key imaging findings

Fatima Ahmad¹, Harita Sivashankar², Andreas Panayiotou³, Marcela de la Hoz Polo⁴,
Saira Haque⁵

¹Radiology department, Royal National Orthopaedic Hospital, Stanmore, London United Kingdom

²Radiology department, Kings College Hospital, Denmark Hill, London United Kingdom

³Alpha Evresis Diagnostic Centre, Bioiatriki Health Group, Nicosia, Cyprus

⁴Everlight Radiology, London, United Kingdom

⁵Radiology department, Kings College Hospital, Denmark Hill, London, United Kingdom

SUBMISSION: 15/02/24 - ACCEPTANCE: 13/03/24

ABSTRACT

Anterior knee pain is common in the paediatric population due to the nature of the immature skeleton and the effects of increased physical activity. Particularly in the growing paediatric knee, there are a wide variety of pathologies and normal variants which can make radiological assessment challenging. Thus, the underlying cause of anterior knee pain is important to identify as it impacts on quality of life. Due to the increased reli-

ance on radiology and technological advancements, we discover more pathology contributing to anterior knee pain. Radiological assessment is the mainstay for investigating causes of knee pain, particularly, plain film, MRI and ultrasound. The purpose of this article is to review the anatomy of the normal knee to demonstrate the structures that are likely to be involved and to illustrate the causes of anterior knee pain in this population.



KEY WORDS

Paediatrics / Knee / Pain / Pathology



CORRESPONDING AUTHOR, GUARANTOR

Fatima Ahmad
Radiology department, Royal National Orthopaedic Hospital
Stanmore, London, United Kingdom, F.ahmad8@nhs.net
07756876105, ORCID: 0009-0001-5184-162

Introduction

This pictorial review aims to disambiguate the paediatric knee and will be presented by pathology according to the surgical compartment. This will be prefaced with a brief overview of anatomy and normal variants.

Normal Anatomy of the Knee

The normal paediatric knee consists of the patellofemoral and medial and lateral tibiofemoral articulations. The joint is stabilised by the surrounding ligamentous, tendinous, muscular structures, bursae and menisci which absorb shock and axial loading forces. Pathology can arise at any of these sites with resultant anterior knee pain. Assessment of patella height and patella translation are demonstrated in Figure 1 which highlights measurements used in the assessment of patella instability.

Congenital

Bipartite patella

Bipartite patella is a normal variant that results from the failure of fusion of the secondary ossification centre of the patella with the main ossification centre and most commonly involves the superolateral pole [1]. Bipartite patella is an uncommon cause of anterior knee pain in the paediatric population and it is usually asymptomatic [2]. Plain film radiography is sufficient to make a diagnosis with the presence of a well-corticated bony fragment usually at the superolateral pole of the patella, best seen in the frontal radiograph. Although the majority of patients are asymptomatic, knee pain may be the result of mechanical instability, stress reaction or injury resulting in disruption of the fibrocartilage between the accessory bone and the main patella ossification centre. For patients with anterior knee pain and a bipartite patella, fluid-sensitive MRI sequences may show bone marrow oedema within the ossicles, indicating it as the cause of knee pain (Fig. 2). The differential diagnosis includes patella fracture, however, in bipartite patella there is continuous cartilage signal across the synchondrosis [1].

Discoid meniscus

Meniscal tears particularly in young athletes contribute to significant morbidity and menisci are therefore key structures to review in paediatric knee MRI. A

discoid lateral meniscus is by far more common than a discoid medial meniscus with an incidence of 0.4% to 17% [3]. Its characteristic features include a body width of 15mm or more on coronal images and the classical 'bow-tie sign' with continuous meniscus on 3 more sagittal slices [4]. While a discoid meniscus may be an incidental finding, it can often be associated with an insidious onset of pain unrelated to trauma [3] and can predispose to degeneration and subsequent tearing of the lateral meniscus. The unstable "Wrisberg variant" is a discoid lateral meniscus associated with a tear or deficiency of the posterior meniscocapsular ligaments with only an attachment with the meniscofemoral ligament of Wrisberg. This can be associated with classical "snapping knee" if unstable. Discoid menisci can easily be appreciated on MRI, particularly on coronal sequences. A ratio of the minimal meniscal width to the maximal tibial width of more than 20% is particularly useful for diagnosis with a sensitivity of 95% [3]. These criteria are particularly useful in paediatric populations where absolute meniscal body measurements can be misleading.

Plica syndromes (Suprapatellar plica)

Plicae are a common incidental finding on imaging and arthroscopy secondary to incomplete resorption of embryonic septae during normal development [5], and as such may be evident within the normal paediatric knee, the vast majority of which are asymptomatic. However, when symptomatic, plica syndromes are an important consideration in the diagnosis of anterior knee pain and may result in traumatic injury and impingement and subsequent chondral damage [6].

Trauma: overuse injuries, apophysitis and fractures

Extensor mechanism injury

The extensor mechanism of the knee comprises the quadriceps muscle, quadriceps tendon, patella and patellar tendon. In the paediatric population, injuries to the extensor mechanism are common and usually secondary to trauma or overuse.

Patellar tendinopathy, as a result of chronic overuse injury, is often referred to as "jumper's knee" due to its association with sports that involve repetitive stress on the patellofemoral joint such as jumping, running and changing direction. Patients usually refer with pain typically felt below the patella and coincident with any activity that involves knee extension. On MRI, this man-

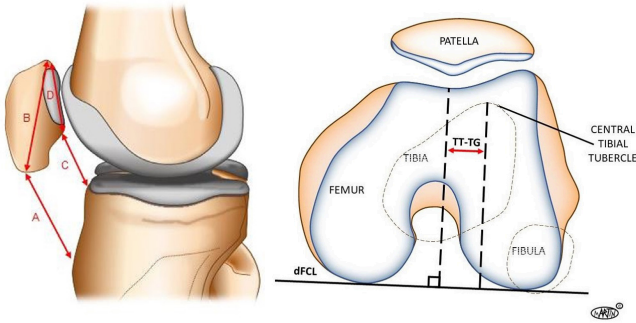


Figure 1a & 1b: Figure 1a demonstrates the assessment of patella height using the Insall-Salvati ratio (A/B) which measures the patella tendon length over the patella length. An alternative assessment includes the Caton-Deschamps index (C/D) which measures the distance between the anterior angle of the tibial plateau to the most inferior aspect of the articular surface of the patella, over the length of the patellar articular surface. Figure 1b demonstrates tibial tubercle-trochlear groove (TT-TG) distance which is used to assess patella translation and instability.



Figure 3: Sagittal PD MR of the left knee demonstrates a well-corticated bone fragment anterior to the tibia as a sequelae of Osgood-Schlatter disease (thin arrow) with hyper trophy of the tibial tuberosity with irregular cortical margins and marrow oedema. The patellar tendon appears thickened at its tibial insertion but remains intact (filled arrow).

ifests as a thickening and oedema-like signal in the proximal third of the patellar tendon with lesions typically occurring in the deep posterior portion of the proximal

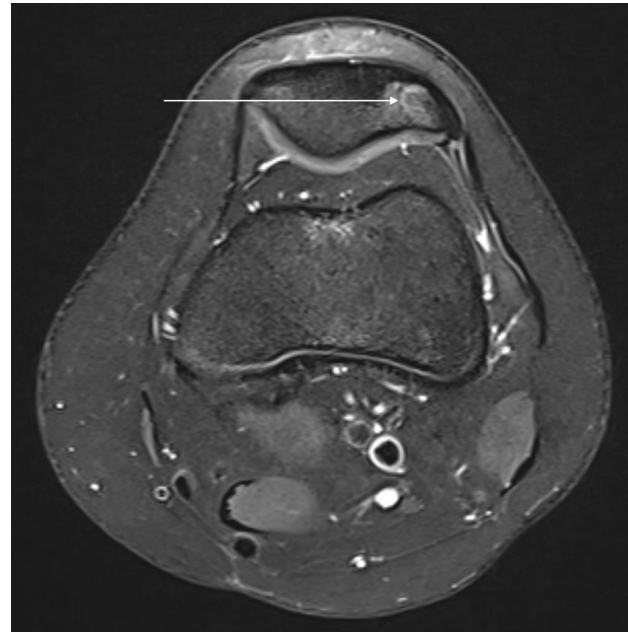


Figure 2: Proton density fat-suppressed (PDFS) axial MR image of the left knee demonstrates a bipartite patella with acute marrow oedema at the site of the synchondrosis suggestive of marrow stress reaction (arrow). No features of instability are identified.



Figure 4: PD-FS sagittal image confirms Sinding-Larsen disease showing thickening of the proximal and posterior part of the patellar tendon with high T2 signal (thin arrow) and adjacent high T2 signal at the inferior pole of the patella (filled arrow).

patellar tendon [7]. Increased signal on fluid-sensitive sequences may also be seen in the inferior patellar pole and adjacent Hoffa's fat pad.

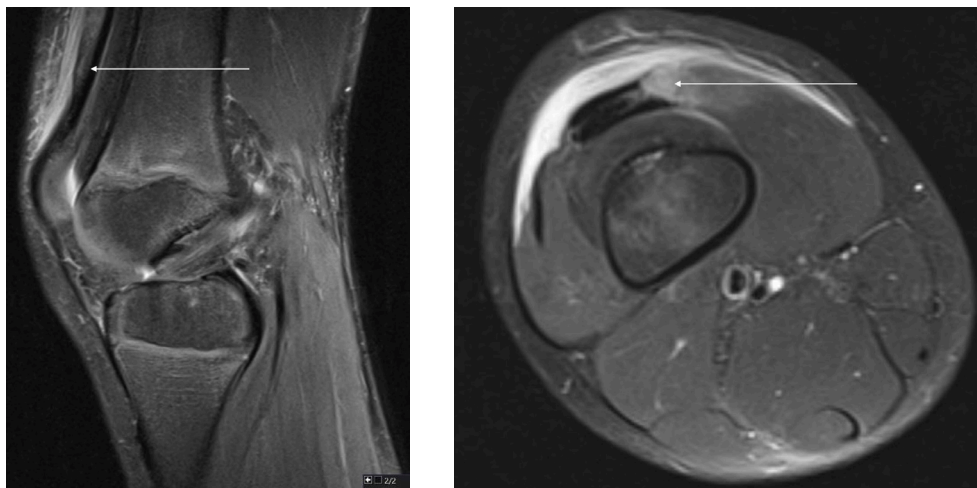


Figure 5a & 5b: Sagittal (Figure 5a) and axial (Figure 5b) PD-FS showing a partial tear of the quadriceps mechanism at the musculotendinous junction, confined to the vastus medialis portion of the tendon.

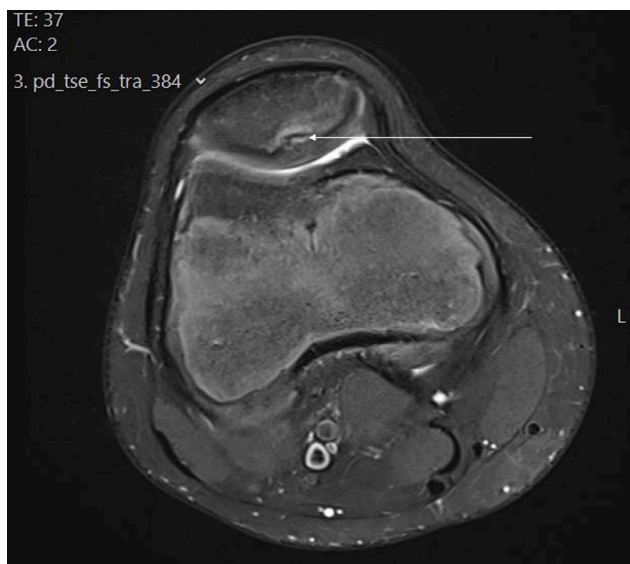


Figure 6: PD-FS axial MR images of the right knee demonstrate an osteochondral abnormality of the dorsal patella with adjacent bone marrow oedema (thin arrow).

Lateral Patellar Dislocation

During lateral patella dislocation, the medial patella impacts the lateral femoral condyle and usually, there is a subsequent medial patellofemoral retinaculum injury, particularly at its femoral condylar insertion. Softer features include high signals within Hoffa's fat pad and loose bodies [8]. Patella alta, trochlear dysplasia and increased tibial tubercle-trochlear groove distance predispose children to lateral patellar dislocation [9, 10]. Lateral trochlear tilt is used for assessing the trochlea



Figure 7: Lateral PD-FS sequence demonstrating irregularity at the inferior patellar pole (thin arrow) in keeping with a sleeve avulsion at the origin of the patellar tendon. The sleeve avulsion tracks anteriorly with oedema tracking adjacent to the anterior patella and into the medial aspect of the distal quadriceps tendon (thick arrow).

and if 1.2 on plain radiographs and >1.5 on MRI indicates patella alta [8].

Osgood-Schlatter Disease

Another overuse injury involving the extensor mechanism of the knee is Osgood Schlatter Disease, also known

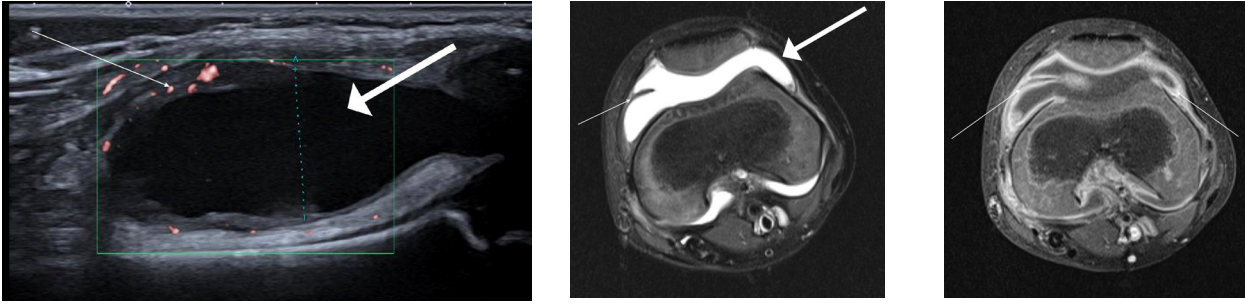


Figure 8a: Ultrasound of the left knee (Figure 8a) highlights a large joint effusion in the suprapatellar region (filled arrow) with florid synovial thickening and hyperaemia (thin arrow). **Figure 8b & 8c:** Axial PD-FS (Figure 8b) and axial T1 FS post-contrast (Figure 8c) MR images of the left knee demonstrate a large knee joint effusion (filled arrow) with florid synovial hypertrophy which demonstrates post-contrast enhancement (thin arrows) most marked in the suprapatellar and patellofemoral regions. Increased vascularity is demonstrated surrounding the knee joint postcontrast.

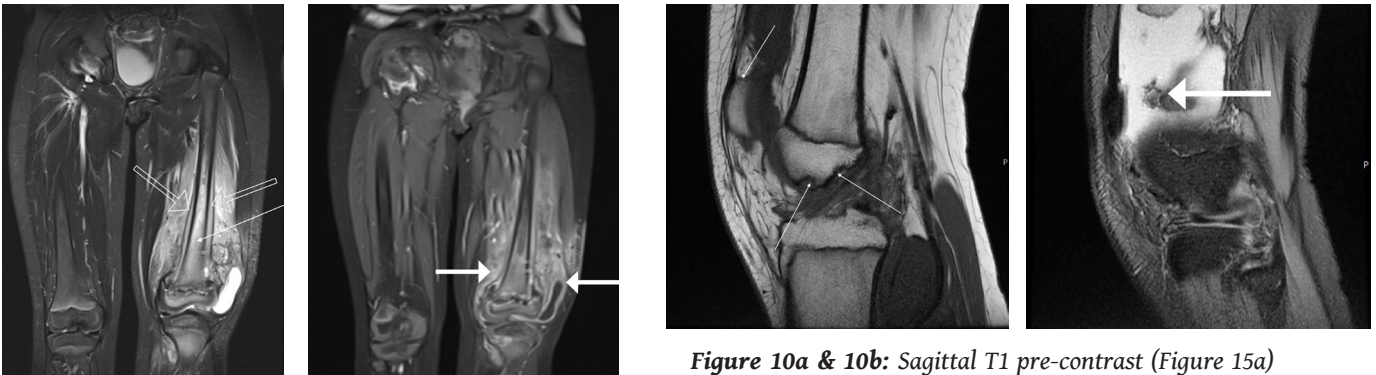


Figure 9a & 9b: T2 coronal and T1 DIXON post-contrast coronal MR images of the left femur demonstrate extensive bone marrow oedema involving the left distal femur, knee and proximal tibia (thin arrow). Soft tissue swelling is seen to extend to involve the anterior compartment of the thigh, most prominently involving the vastus intermedius. There is evidence of cortical breach and marked periosteal reaction (unfilled arrows) with a large knee joint effusion and post-contrast enhancement (filled arrow). This appearance is consistent with septic arthritis of the left knee with soft tissue extension and osteomyelitis within the distal femur.

Figure 10a & 10b: Sagittal T1 pre-contrast (Figure 15a) and T2* (Figure 15b) images show synovitis with enhancement of the synovial tissue. GRE images (Figure 15b) demonstrate low signal within the synovial fronds (filled arrow) and T1 images (15a) show erosions in the central ridge of patellar and trochlear apex (thin arrows).

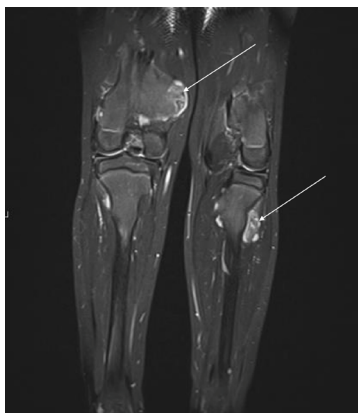


Figure 11: A 7-year-old male with a history of familial diaphyseal aclasis presented with restricted movement and knee pain. Coronal STIR sequences of the knees show multiple osteochondromas of the femurs and tibiae (arrows). No aggressive features. The peroneal nerve is in close proximity to the proximal fibular osteochondroma.

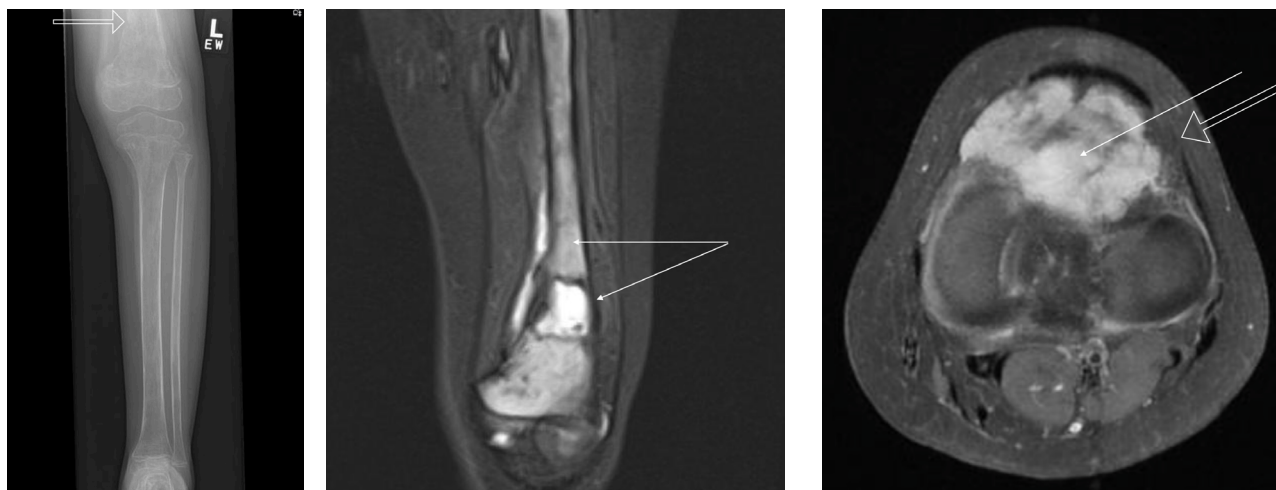


Figure 12a & 12b: Acute lymphocytic leukaemia in a 5-year-old with a 6-month history of left knee pain. The AP radiograph (Figure 12a) demonstrates a pathological fracture of the left distal femur with cortical destruction and associated osteopenia. Coronal STIR (Figure 12b) highlights diffusely heterogeneous bone marrow signal (thin arrows).

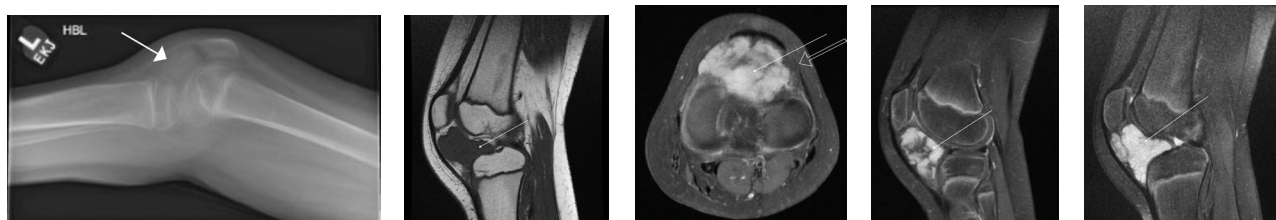


Figure 13 a – e: Lateral radiograph (Figure 13a) of the left knee demonstrates heterogeneity and ectopic calcification posterior to the patellar tendon in Hoffa's fat pad (filled arrow). T1 weighted sagittal (Figure 13b) MR of the knee in the same patient, post-contrast T1 fatsat axial (Figure 13c) and sagittal (Figure 13d), and sagittal PD-FS sequences (Figure 13e) show a lobulated soft tissue mass 4cm (CC) x 4.4cm (T) x 3.6cm (AP) centred in the infrapatellar fat pad with heterogeneous enhancement (thin arrows). In Figure 13c, it infiltrates and extends beyond the medial patellofemoral retinaculum (unfilled arrow).

as tibial tubercle apophyseal injury or apophysitis. Like patellar tendinopathy, it is a cause of anterior knee pain in adolescents and is due to repeated traction on the immature tibial tuberosity [11]. Avulsion fractures may be seen alongside this, however fragmentation of the tibial apophysis is a normal variant and special care must be taken not to overcall these as disease. Usually, soft tissue swelling on plain radiograph, if present, can be helpful in supporting the diagnosis. However, clinical history and correlation is important to diagnose this condition. MRI can be helpful in detecting early disease and for monitoring progression. MRI can show partial avulsion of the secondary ossification centre which is pulled proximally in early disease and completely separated in later stages (Fig. 3) [12].

Sinding-Larson-Johansson Syndrome

Sinding-Larson-Johansson disease is another common cause of anterior knee pain in the paediatric population, particularly in children who have had rapid growth spurts, most commonly aged 10 to 14 years. It is an osteochondrosis of the inferior pole of the patellar and often bilateral [13]. Incidence is unknown and aetiology is believed to be related to overuse [14]. It is caused by traction of the patellar tendon at its insertion on the inferior pole of the patellar and can be differentiated from patellar tendinopathy by the presence of bone marrow oedema in the patellar on fluid sensitive MRI sequences (Fig. 4) [11]. The absence of cartilaginous involvement on MRI and the non-acute nature of presentation distinguishes this from patellar sleeve avulsion which can



Figure 14a & 14b: Sagittal PD (Figure 14a) and PD-FS (Figure 14b) MR images of the right knee highlight extensive marrow oedema through the lateral femoral condyle with a non-displaced subchondral fracture likely representing osteonecrosis (thin arrows). There are multiple serpiginous medullary lesions within the proximal patellar pole and femoral shaft consistent with medullary infarcts (unfilled arrows).

have a similar radiographic appearance [13].

Quadriceps tendinopathy and rupture

Quadriceps tendinopathy is much less common than patellar tendinopathy due to greater tensile strength, mechanical advantage and better blood supply to the tendon [15]. In the paediatric age group, it is an uncommon cause of anterior knee pain. When present, it can manifest as pain at the proximal pole of the patella and can be encountered with activities that involve jumping, climbing, kicking or running. The most common site of injury is at the distal attachment of the quadriceps tendon on the patella (Fig. 5a) [11]. MRI offers the best definition of the quadriceps tendon and its layers due to its superior soft tissue contrast resolution and fluid sensitive sequences can show tendon signal changes at the insertion site or oedema within the distal attachment (Fig. 5b).

Fractures

Salter-Harris Fractures

Trauma in the paediatric population is variable and can result in different patterns of injury, with Salter-Harris fractures encompassing the fracture patterns affecting the growth plates. Salter-Harris Type II fractures represent the most common distal femoral physical fracture. Assessment of fracture extension to the physis is particularly important, due to the potential

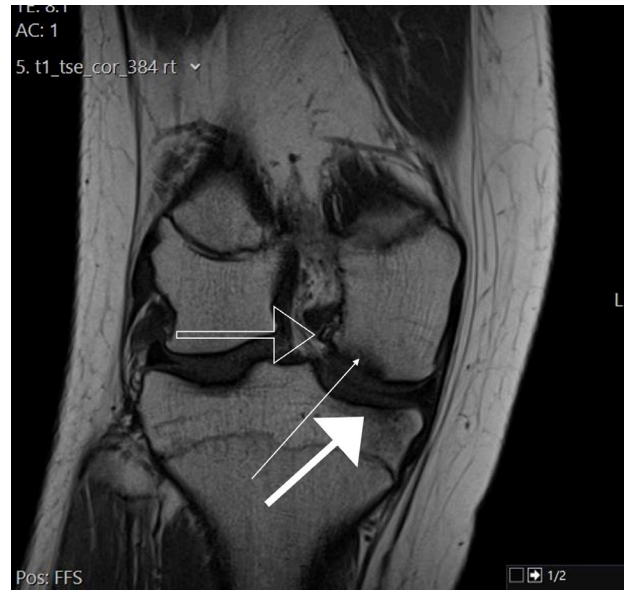


Figure 15: Coronal image of the right knee demonstrates an osteochondral fracture of the posteromedial femoral condyle with adjacent bone marrow oedema (thin arrow) and a loose body in the patellofemoral joint space (unfilled arrow). There is associated contrecoup injury to the medial tibial epiphysis with bone contusion and trabecular disruption (filled arrow)

implications on further growth and bone development and risk of entrapment of structures [16,17]. Salter-Harris fractures of the proximal tibia are uncommon due to the epiphysis being protected by the collateral ligaments which insert distal to the metaphysis [18]. Thus, Salter-Harris fractures of the proximal tibia are usually the result of significant trauma [19].

Stress fractures

The patella is the largest sesamoid bone in the body and, although it does not contribute to the weight bearing mechanism, stress fractures can develop with activities that involve repetitive high tensile forces, twisting and bending and can occur in children with a predisposition to fractures (Fig. 6). Such fractures can be easily misdiagnosed and where they usually heal well, a delayed union may develop, or fragments can separate necessitating operative management [20]. The diagnosis should be suspected after excluding other pathology. On imaging, plain radiographs may be normal although serial radiographs may show the presence of a longitu-

dinal or transverse fracture.

Patellar sleeve avulsion fracture

These occur due to quadriceps muscle contraction usually from jumping [21]. On plain film, fragments of bone may be seen superior or inferior to the patella, but this may not always be seen as, rather than a bone avulsion, it is the periosteum of the patella which is detached (Fig. 7) [22]. MRI more accurately can identify this type of injury and can show the separation of the patellar ligament [21,23].

Inflammatory

Juvenile idiopathic arthritis (JIA)

JIA represents one of the most common paediatric arthritis presenting with persistent joint symptoms for more than 6 weeks. The most frequent symptoms of a hot painful joint may be easily mistaken for a variety of pathologies and therefore MR is the mainstay imaging, not only for diagnosis but monitoring disease progression and treatment response. Imaging findings of joint effusion, synovial proliferation, and the formation of pannus are often visualised (Fig. 8) with the knee being the most typically affected joint with specific features of patellar tendon enthesitis, infrapatellar fat pad enhancement and flexion contracture in longstanding disease [6,24].

Infrapatellar bursitis

Mechanical overuse and the repetitive placement of excessive compressive strain on the extensor mechanism structures may result in bursitis, particularly seen in young athletes. Little or no prepatellar fluid is usually seen in the normal paediatric knee joint and thus the accumulation of fluid, synovitis and bursal thickening should alert the radiologist [6]. Features may be particularly dramatic in chronic cases with a mass-like structure extending beyond the patellar margins. However, the findings may be difficult to distinguish from infection [25,26].

Infectious

Septic Arthritis

Septic arthritis requires prompt clinical diagnosis with confirmation through fluid aspiration and culture. It usually relates to haematogenous spread, local extension from soft tissues or osseous infection, or secondary to penetrating injury and reaction secondary to foreign

bodies, especially in the paediatric population [6]. On MR, low T1 signal in the subchondral bone is noted, with corresponding high T2 signal indicative of subchondral oedema; pericapsular oedema can also be seen (Fig. 9a). Post contrast, T1 shows synovial enhancement secondary to synovitis and pericapsular enhancement (Fig. 9b).

Benign Neoplasms

Many benign tumours are seen within the paediatric knee including non-ossifying fibromas which predominate as benign bone lesions [27], however, only a few can cause anterior knee pain.

Most of the anterior knee is lined with synovium, therefore the neoplasm that most commonly causes anterior knee pain in the paediatric population is tenosynovial giant cell tumour, which affects the synovium and tendon sheaths [28]. Initially, it presents as swelling, and as it expands, joint pain and restricted movement follow [29]. This condition can be evaluated with a plain film which can show a soft tissue mass, joint effusion, or in advanced stages, bone erosion [30]. MRI remains the gold standard for evaluation of this tumour. MRI features include proliferation of the synovium, joint effusion and haemosiderin deposition [31]. The tumour displays low signal on T1 and T2 weighted sequences and variable enhancement (Fig. 10) [30]. Gradient echo is diagnostic as it shows a blooming artefact which is secondary to haemosiderin deposition by the tumour and is a classic feature.

Osteochondromas, being the commonest benign tumour overall representing 20-50% of all benign bone tumours, can also cause knee pain [32]. They can be multiple, suggesting the syndrome hereditary multiple exostoses. The complications of osteochondromas include fractures, compression of local structures, bursitis or malignant transformation [33]. Plain film remains ideal for diagnosing the presence of an osteochondroma. However, MRI provides the highest yield in identifying complications associated with osteochondromas, and delineation of the cartilage cap, oedema, and involvement of local structures (Fig. 11) [33].

Malignant neoplasms

Osteosarcoma, Ewing sarcoma, and rhabdomyosarcoma are the most common malignant musculoskeletal tumours in the paediatric population [34].

Osteosarcoma presents commonly with pain and swelling [35] and 50% occur around the knee. Radiographs can identify permeative pattern of destruction and periosteal reaction whilst MR can depict skip lesions, soft tissue extent and if in close proximity to neurovascular structures [36]. Ewing's sarcoma can also present with pain but is more highly susceptible to metastasis [37]. Rhabdomyosarcoma is the most common soft tissue sarcoma in children (38). It usually demonstrates iso to hyperintense on T1 due to haemorrhage and necrosis and heterogeneous enhancement post-contrast [39].

Other malignancies causing pain, most often affecting the knee joint include leukaemias, particularly acute lymphocytic leukaemia [40]. Its clinical presentation is usually with fever, pallor and bone pain [41]. Furthermore, a pathological fracture may even be the initial presentation of leukaemias radiologically (Fig. 12a) [42]. Features of bone infiltration are usually seen on plain film and MRI. On plain film, this may appear as cortical irregularity, permeative bone destruction and pathological fracture. MRI more accurately demonstrates the infiltrative bone spread with homogenous low T1 signal with no normal fatty marrow, and a soft tissue mass (Fig. 12b) [43].

Synovial sarcomas usually present as a slow-growing peri-articular or intra-articular mass which may eventually cause pain or joint contractures [44]. Frequently, they affect joints of the lower limbs including the knee joint [44,45]. Although MRI pre and post-contrast remains the main imaging modality for diagnosis, plain film is beneficial in initially identifying calcification or bony remodelling (Fig. 13a-e).

Vascular

Avascular necrosis and osteonecrosis in sickle cell disease

Avascular necrosis occurs when there is an interruption of the blood supply to the subchondral bone and tends to affect the epiphyses of long bones including those around the knee [46]. Bone infarction refers to diaphyseal or metaphyseal osteonecrosis. Haemoglobinopathies such as sickle cell disease and thalassemia are some of the conditions which may cause osteonecrosis. Bone marrow changes, which are best seen on MR, include a well-demarcated lesion on T1 which is hypointense (Fig. 14a) and a serpiginous double line sign on T2 which is described as an inner high T2 sig-

nal line delineating granulation tissue and a low signal outer line T2 (Fig. 14b) This line has been edited. This is considered as pathognomonic [47]. Rim enhancement is seen post-contrast.

Miscellaneous

Osteochondritis dissecans

Osteochondritis dissecans often presents insidiously with a history of joint locking secondary to intra-articular loose bodies and knee pain on mobilisation. Its aetiology in the paediatric population is thought to be due to repetitive injury or trauma, subsequent osteochondral fracture and subchondral avascular necrosis with the formation of osteochondral defects and loose fragments leading to instability (Fig. 15) [21]. Osteochondritis dissecans are usually present around the ages of 12 to 13 years and are often asymmetrical. A history of trauma is found in more than 50% of cases [48]. As children have a greater propensity to heal, a better prognosis is seen in paediatric patients in comparison to adults [49]. However, awareness of the variants of normal ossification is imperative to prevent misdiagnosis as osteochondritis dissecans.

Conclusion

There is a wide variety of causes of anterior knee pain, which ranges from normal variants of ossification, overuse overuse-related injuries, to benign and malignant conditions. Referred pain from hip joint pathology and lumbar pain should importantly be taken into account when assessing a child with anterior knee pain. Imaging remains crucial in the diagnosis and deciphering of the cause to ensure accurate diagnosis and management of these processes in the paediatric population. Radiographs are usually the initial imaging approach in the diagnostic algorithm. However, many of the pathological processes need further investigation with ultrasound or MRI which yield better depiction of the structures and compartments involved. Radiologists should be particularly aware of the differential diagnosis, and along with the clinical history, aid in the selection of the best modality of choice to arrive at the correct diagnosis. **R**

Acknowledgements

Martin Mckeown, the illustrator, for the schematic drawings.

REFERENCES

1. Akdag T, Guldogan E S, Coskun H, et al. Magnetic resonance imaging for diagnosis of bipartite patella: usefulness and relationship with symptoms. *Polish Journal of Radiology* 2019; 84.e491–e497. doi:10.5114/pjr.2019.911631.
2. Berger R, Yen Y. Bipartite Patella - Pediatrics - Orthobullets. Orthobullets.com. <https://www.orthobullets.com/pediatrics/4049/bipartite-patella>. Published 2021.
3. Yaniv M, Blumberg N. The discoid meniscus. *Journal of Children's Orthopaedics* 2007; 1(2):89–96. doi:10.1007/s11832-007-0029-1.
4. Birchard Z, Herron T, Tuck JA. Discoid Meniscus. 2023 Mar 6. In: StatPearls [Internet]. Treasure Island (FL): StatPearls Publishing; 2024 Jan-. PMID: 29261944.
5. García-Valtuille R, Abascal F, Cerezal L, et al. Anatomy and MR imaging appearances of synovial plicae of the knee. *Radiographics* 2002;22(4):775–784.
6. Flores DV, Mejía Gómez C, Pathria M N. Layered Approach to the Anterior Knee: Normal Anatomy and Disorders Associated with Anterior Knee Pain. *Radiographics* 2018; 38(7): 2069–2101. doi:10.1148/rg.2018180048.
7. Warden S, Brukner P. Patellar tendinopathy. *Clin Sports Med.* 2003;22(4):743–759. doi:10.1016/s0278-5919(03)00068-1
8. Elias DA, White LM, Fithian DC. Acute lateral patellar dislocation at MR imaging: injury patterns of medial patellar soft-tissue restraints and osteochondral injuries of the inferomedial patella. *Radiology.* 2002; 225(3):736–43. doi: 10.1148/radiol.2253011578. PMID: 12461254.
9. Zaidi A, Babyn P, Astori I, et al. MRI of traumatic patellar dislocation in children. *Pediatr Radiol* 2006; 36(11):11631170.
10. Dickens AJ, Morrell NT, Doering A, et al. Tibial Tubercle-Trochlear Groove Distance: Defining Normal in a Pediatric Population. *J Bone Joint Surg Am* 2014; 96(4):318–324. doi:10.2106/jbjs.m.00688.
11. Ladenhauf HN, Seitlinger G, Green DW. Osgood-Schlatter disease: a 2020 update of a common knee condition in children. *Curr Opin Pediatr.* 2020;32(1):107–112. doi:10.1097/mop.0000000000000842
12. Hirano A, Fukubayashi T, Ishii T, et al. Magnetic resonance imaging of Osgood-Schlatter disease: the course of the disease. *Skeletal Radiol.* 2002 ;31(6):334–42. doi: 10.1007/s00256-002-0486-z.
13. Cleveland Clinic. Sinding-Larsen-Johansson Syndrome: Diagnosis & Treatment. Cleveland Clinic. <https://my.clevelandclinic.org/health/diseases/22530-sinding-larsen-johansson-slj-syndrome>. Published 2022. Accessed August 26, 2022.
14. Alassaf N. Acute presentation of Sinding-Larsen-Johansson disease simulating patella sleeve fracture: A case report. *SAGE Open Med Case Rep.* 2018 Sep doi: 10.1177/2050313X18799242.
15. King D, Yakubek G, Chughtai M et al. Quadriceps tendinopathy: a review, part 2— classification, prognosis, and treatment. *Ann Transl Med.* 2019;7(4):72. doi:10.21037/atm.2019.01.63
16. Arkader A, Warner WC Jr, Horn BD, et al. Predicting the outcome of physeal fractures of the distal femur. *J Pediatr Orthop* 2007; 27(6):703–708.
17. Czitrom A A, Salter R B, Willis R B. Fractures involving the distal epiphyseal plate of the femur. *International Orthopaedics.* 1981;4(4):269–277.
18. Clement ND, Goswami A. Salter-Harris II injury of the proximal tibial epiphysis with both vascular compromise and compartment syndrome: a case report. *J Orthop Surg Res* 2009; 4:23. doi:10.1186/1749-799X4-23.
19. Verzin EJ, Kealey D, Adair A, et al. Salter-Harris type I fracture of the proximal tibial epiphysis. *Ulster Med J* 2001; 70(2):136–138.
20. Kizaki K, Yamashita F, Funakoshi N. Serial Radiographs Showing Progression of a Patellar Stress Fracture and Beneficial Surgical Technique for a Displaced Patellar Stress Fracture. *Knee Surg Relat Res* 2018; 30(1):89–92. doi:10.5792/ksrr.17.044.
21. Schmidt-Hebbel A, Eggers F, Schütte V. et al. Pa-

- tellar sleeve avulsion fracture in a patient with Sinding-Larsen-Johansson syndrome: a case report. *BMC Musculoskelet Disord* 2020; 21(1). doi:10.1186/s12891-020-03297-z.
22. Hunt DM, Somashekar N. A review of sleeve fractures of the patella in children. *Knee* 2005; 12(1):3-7. doi:10.1016/j.knee.2004.08.002.
 23. Boushnak MO, Moussa MK, Abed Ali AA, et al. Patellar Sleeve Fracture in an Eight-Year-Old Girl. *Cureus* 2020; 12(9):e10345. doi:10.7759/cureus.10345
 24. Sanchez R, Strouse P J. The knee: MR imaging of uniquely pediatric disorders. *Magn Reson Imaging Clin N Am* 2009; 17(3):521-537. doi:10.1016/j.mric.2009.03.008.
 25. Donahue F, Turkel D, Mnaymeh W, et al. Hemorrhagic prepatellar bursitis. *Skeletal Radiol* 1996;25(3):298-301.
 26. Steinbach LS, Stevens K J. Imaging of cysts and bursae about the knee. *Radiol Clin North Am* 2013; 51(3):433-454.
 27. Rammanohar J, Zhang C, Thahir A, et al. Imaging of Non-ossifying Fibromas: A Case Series. *Cureus* 2021; 13(#): e14102. doi:10.7759/cureus.14102.
 28. Fecek C, Carter KR. Pigmented Villonodular Synovitis. 2023[online] PubMed. Available at: <https://www.ncbi.nlm.nih.gov/books/NBK549850/>.
 29. Fałek A, Niemunis-Sawicka J, Wrona K, et al. Pigmented villonodular synovitis. *Folia Med Cracov.* 2018;58(4):93-104. PMID: 30745604.
 30. Tritschler P, Baudrez, V, Mutijima, E. Diffuse Pigmented Villonodular Synovitis of the Subtalar Joint. *J Belg Soc Radiol.* 2018; 102(1):11. doi:10.5334/jbsr.1477.
 31. Cheng XG, You YH, Liu W, et al. MRI features of pigmented villonodular synovitis (PVNS). *Clin Rheumatol* 2004; 23(1):31-34 doi:10.1007/s10067-003-0827-x.
 32. Garcia RA, Inwards CY, Unni KK. Benign bone tumors--recent developments. *Semin Diagn Pathol* 2011; 28(10):73-85. doi:10.1053/j.sem-dp.2011.02.013.
 33. Motamedi K, Seeger LL. Benign Bone Tumors. *Radiologic Clinics of North America* 2011; 49(6):1115-1134. doi:10.1016/j.rcl.2011.07.002.
 34. Arndt CA, Rose PS, Folpe AL, et al. Common Musculoskeletal Tumors of Childhood and Adolescence. *Mayo Clin Proc*, 2012; 87(5):475-487. doi:10.1016/j.mayocp.2012.01.015.
 35. Pan KL, Chan WH, Chia YY. Initial Symptoms and Delayed Diagnosis of Osteosarcoma around the Knee Joint. *J Orthop Surg*, 2010; 18(1):55- 57. doi:10.1177/230949901001800112.
 36. Kundu ZS. Classification, imaging, biopsy and staging of osteosarcoma. *Indian J Orthop*, 2014; 48(3):238-246. doi:10.4103/0019-5413.132491.
 37. Durer S, Gasalberti DP, Shaikh H. Ewing Sarcoma. [Updated 2024 Jan 8]. In: StatPearls [Internet]. Treasure Island (FL): StatPearls Publishing; 2024 Jan-. Available from: <https://www.ncbi.nlm.nih.gov/books/NBK559183/>
 38. Laor T. MR imaging of soft tissue tumors and tumor-like lesions. *Pediatr Radiol* 2004; 34(1):24-37. doi:10.1007/s00247-003-1086-3.
 39. Schoot RA, McHugh K, van Rijn RR, et al. Response Assessment in Pediatric Rhabdomyosarcoma: Can Response Evaluation Criteria in Solid Tumors Replace Three-dimensional Volume Assessments? *Radiology* 2013; 269(3):870-878. doi:10.1148/radiol.13122607.
 40. van der Have N, Nath SV, Story C, et al. Differential diagnosis of paediatric bone pain: Acute lymphoblastic leukemia. *Leuk Res* 2012; 36(4):521-523. doi:10.1016/j.leukres.2012.01.001.
 41. Onciu M. Acute Lymphoblastic Leukemia. *Hematology/Oncology Clinics of North America* 2009; 23(4):655-674. doi:10.1016/j.hoc.2009.04.009.
 42. Tannenbaum MF, Noda S, Cohen S, et al. Imaging Musculoskeletal Manifestations of Pediatric Hematologic Malignancies. *Am J Roentgenol* 2020; 214(2):455-464. doi:10.2214/ajr.19.21833.
 43. Marshall RA, Mandell JC, Weaver MJ, et al. Imaging Features and Management of Stress, Atypical, and Pathologic Fractures. *RadioGraphics* 2018; 38(7):2173-2192. doi:10.1148/rg.2018180073.
 44. Chotel F, Unnithan A, Chandrasekar CR, et al. Variability in the presentation of synovial sarcoma in children. *J Bone Joint Surg Br*, 2008; 90(8):1090-1096. doi:10.1302/0301-620x.90b8.19815.

45. Eilber FC, Dry SM. Diagnosis and management of synovial sarcoma. *J Surg Oncol*, 2008; 97(4):314–320. doi:10.1002/jso.20974.
46. Lespasio M J, Sodhi N, Mont M A. Osteonecrosis of the Hip: A Primer. *Perm J*. 2019; 23:18-100. doi: 10.7812/TPP/18-100. PMID: 30939270; PMCID: PMC6380478.
47. Tang YM, Jeavons S, Stuckey S, et al. MRI features of bone marrow necrosis. *AJR. AmJ Roentgenol* 2007; 188(2):509– 514. doi:10.2214/AJR.05.0656.
48. Shea KG, Jacobs JC, Carey JL, et al. Osteochondritis Dissecans Knee Histology Studies Have Variable Findings and Theories of Etiology. *Clinical Orthopaedics & Related Research* 2013; 471(4):1127–1136. doi:10.1007/s11999-012-2619-6.
49. Kijowski R, Blankenbaker DG, Shinki K, et al. Juvenile versus Adult Osteochondritis Dissecans of the Knee: Appropriate MR Imaging Criteria for Instability. *Radiology* 2008; 248(2):571–578. doi:10.1148/radiol.2482071234



READY - MADE
CITATION

Fatima Ahmad, Harita Sivashankar, Andreas Panayiotou, Marcela de la Hoz Polo, Saira Haque. Anterior knee pain in paediatrics: Key imaging findings. *Hell J Radiol* 2024; 9(1): 44-55.